





Article

Image Processing Technique for Enhanced Combustion Efficiency of Wood Pellets

Thomas Gasperini , Andrea Pizzi , Lucia Olivi, Giuseppe Toscano , Alessio Ilari *  and Daniele Duca * 

Department of Agricultural, Food and Environmental Sciences, Marche Polytechnic University, Via Breccie Bianche, 60131 Ancona, Italy; t.gasperini@univpm.it (T.G.); g.toscano@univpm.it (G.T.)

* Correspondence: a.ilari@univpm.it (A.I.); d.duca@univpm.it (D.D.)

Abstract: The combustion efficiency of wood pellets is partly affected by their average length. The ISO 17829 standard defines the methodology for assessing the average length of sample pellets, but the method does not always lead to representative data. Furthermore, a standard analysis is time-consuming as it requires manual measurement of the pellets using a caliper. This paper, whilst evaluating the effect of pellet length on combustion efficiency, proposes a pending-patented dimensional image processing method (DIP) for assessing pellet length. DIP allows the dimensional data of grouped and stacked pellets to be obtained by exploiting the shadows produced by pellets when exposed to a light source, assuming that different-sized pellets produce different shadows. Thus, the proposed method allows for the extraction of dimensional information from non-distinct objects, overcoming the reliance of classical image processing methods on object distance for effective segmentation. Combustion tests, carried out using pellets varying only in length, confirmed the influence of length on combustion efficiency. Shorter pellets, compared to longer ones, significantly reduced CO emissions by up to 94% (mg/MJ). However, they exhibited a higher fuel mass consumption rate (kg/h), with an increase of up to 22.8% compared to the longest sample. In addition, longer pellets produced fewer but larger shadows than shorter ones. Further studies are needed to correlate the number and size of shadows with samples' average length so that DIP could be implemented in stoves and programmed to communicate with the control unit and automatically optimize the setting in order to improve combustion efficiency.



Citation: Gasperini, T.; Pizzi, A.; Olivi, L.; Toscano, G.; Ilari, A.; Duca, D. Image Processing Technique for Enhanced Combustion Efficiency of Wood Pellets. *Energies* **2024**, *17*, 6144. <https://doi.org/10.3390/en17236144>

Academic Editors: Claudia Toro and Chiara Martini

Received: 14 November 2024

Revised: 29 November 2024

Accepted: 3 December 2024

Published: 5 December 2024



Copyright: © 2024 by the authors. Licensee MDPI, Basel, Switzerland. This article is an open access article distributed under the terms and conditions of the Creative Commons Attribution (CC BY) license (<https://creativecommons.org/licenses/by/4.0/>).

Keywords: solid biofuel; stove emissions; low-cost sensor; image processing; binarization; pellet length; precision bioenergy

1. Introduction

The European interest in renewable energy, reflected by EU Directive 2009/28/EC and, today, renewed through the update of the Green Deal, has led to an expansion of the market of renewable energies and solid biofuels [1,2]. Among them, wood pellets have been one of the most successful and most used in household heating [3,4]. In fact, although some countries experienced a decrease in pellet production, such as Italy, which saw a 4.4% drop from 450 thousand tons to 430 thousand tons between 2014 and 2023, the overall pellet production in Europe increased significantly by 79.2%, rising from 484 thousand tons to 867 thousand tons [5].

However, whilst representing an important energy source, solid biofuels are well known as the cause of significant emissions of air pollutants in urban and rural areas [6]. For this purpose, many experimental and modelling studies have been conducted to obtain information on pollutant dispersion for monitoring and assessing possible long-term strategies to reduce air pollution in cities. Over the years, worldwide regulations have imposed progressively restrictive thresholds for atmospheric pollutant concentrations [7]. Therefore, in the context of the development of the biomass market, there also has been an

increased focus on the monitoring of biomass quality parameters, specifically of pellets' overall quality.

The ISO 17225-2 standard defines the pellet quality classes and thresholds for chemical, energetic, and physical parameters [8]. The latter include geometric parameters such as diameter and length. Specifically, ISO 17225-2 indicates that pellets should not be shorter than 3.15 mm and longer than 40 mm. ISO 17829 outlines the procedure for measuring the diameter and length of pellet samples using a caliper [9]. However, the standard methodology is time-consuming, therefore leading to the analysis of a limited number of pellets, which may result in non-representative data [10,11].

Geometrical parameters have numerous effects on pellets' overall quality. Gilvari et al. and Lisowski et al. investigated the effect of length on pellets' durability [12,13], whilst Pradhan et al. found an inverse relation between pellet's length and its bulk density [14]. A number of studies focused on the assessment of pellet length's influence on combustion efficiency, the latter playing a crucial role in the quality of flue gas emissions from domestic heating systems [15]. Wöhler et al. highlighted a correlation between pellet length, and carbon monoxide (CO) and particulate (PM) emissions [16]. Moreover, Mack et al. found that longer pellets lead to a reduction in fuel mass flow and an increase in lambda values, and hence lower combustion efficiency [17]. Therefore, monitoring pellet's overall quality and geometrical parameters is a key element in optimizing its use and reducing environmental impacts [18].

In recent years, studies have been proposing alternative methods to those defined by the standard for rapid and accurate monitoring of solid biofuel's overall quality. For densified biofuels, such as briquettes and pellets, computer vision and image processing are some of the most widely used alternative methods. For instance, Igathinathane et al. developed thresholding image processing software to assess the fine content in industrial environments during pellet production [19], while Chaloupková et al. applied image processing techniques to assess the size and densification of particles composing briquettes [20].

A number of studies have also researched the application of image processing techniques for monitoring pellet length [10,21,22]. However, to the best of author's knowledge, there are no studies suggesting methods to assess the size of pellets placed in bulk. When using traditional segmentation and thresholding methods, bulk analysis appears difficult and unreliable, as pellets placed transversely within the bulk lead to length measurement errors, making this method not applicable on production lines or within heating systems. In this context, the proposed principle addresses the limitations of segmentation techniques for objects that are not clearly separated or parallel to the camera by analyzing shadows cast by pellets and establishing a reliable correlation between shadow size and pellet size.

In this regard, this paper analyses the effect of pellets differing only in length on combustion quality and proposes an innovative approach based on image processing, which allows for the dimensional analysis of unsorted pellets, placed in bulks. The proposed method is currently undergoing patenting.

2. Materials and Methods

This research consists of two separate lines of work. The former aimed to assess the influence of pellet length on combustion efficiency, as suggested in prior papers [16,17], whilst the latter evaluated a prototypal system which allows for the measurement of pellet length in bulk via image processing.

The prototypal system differs significantly from the standard measuring methodology for pellet length, which involves the use of a caliper [9]. Specifically, the principle behind the prototype is to obtain dimensional data of the samples by exploiting the shadows generated by the pellets when subjected to a light source, assuming that different-sized pellets generate different shadows.

Therefore, pellets of different lengths were produced using the same raw material, thus attempting to limit the variables which affect combustion efficiency [23]. Prior to the

combustion tests and measurement by the prototype system, the chemical, physical, and energetical parameters of the pellet samples were assessed.

Detailed descriptions of each methodology step are presented in the following sections.

2.1. Sample Preparation

The production of wooden pellets took place at Enerlegno (Forlì, FC), a local Italian pellet company equipped with a horizontal die pelletizer. The raw material used throughout the production process was spruce (*Picea abies*) sawdust, being one of the most widely available and used species in pellet production.

Using the same raw material whilst varying the distance between the horizontal die and the pelletizer's knives allowed pellets which mostly differed in length to be obtained. Specifically, the knives were placed at a distance of 25, 35, and 45 mm from the die, producing three types of samples: predominantly short pellets (Sp), medium-length pellets (Mp), and predominantly long pellets (Lp). About 50 kg of each type of pellet was produced. Knife distances were chosen according to previous experimental tests.

To assess the geometrical parameters of Sp, Mp and Lp, sample homogenization and reduction were carried out according to the ISO 21945 methodology [24], producing three sub-samples, 5 kg each. Thus, a total of 300 randomly selected pellets from each sub-sample were measured through the use of a digital Maurer caliper (accuracy 0.01 mm), according to the ISO 17829 methodology.

Furthermore, the overall quality of Sp, Mp and Lp was assessed by measuring the following parameters: moisture content (MC, ISO 18134-2 [25]); ash content (ISO 18122 [26]); net, higher, and lower heating values (NCV, HCV, and LCV respectively, ISO 18125 [27]); chemical composition (C, H, N content—ISO 16948 [28]); chlorine and sulfur content (Cl, S—ISO 16994 [29]); durability (ISO 17831-1 [30]); and fine content (ISO 18846 [31]).

Lastly, further sample reduction was carried out on Sp, Mp, and Lp by manually selecting pellets in order to obtain sub-samples (Sp2, Mp2, and Lp2) with distinctly different average lengths. The latter sub-samples were used to test the prototypal dimensional image processing measuring system (DIP). Lastly, 150 pellets randomly selected from Sp2, Mp2, and Lp2 were measured using a caliper.

2.2. Combustion Tests

The combustion efficiency of Sp, Mp, and Lp was evaluated through the use of a pellet stove with 10 kW nominal heating capacity (mod. 6000 Caminetti Montegrappa, Pove del Grappa, Italy) and an emission analyzer (Vario plus, MRU, Humble, TX, USA). The emission analyzer was connected directly to the chimney at a distance of 1.5 m from the stove exhaust pipe, allowing for continuous monitoring of the flue gases' composition and temperature. Furthermore, the stove was placed upon an industrial scale (accuracy 5 g) to assess the samples' mass flow rate (MFR, kg/h) during each combustion test. The experimental setup is shown in Figure 1.

Trends in the emissions of carbon monoxide (CO), nitrogen oxides (NO_x), lambda (λ) and flue gas temperature (°C) were measured via the MRU analyzer, while varying the stoves' default programs (F3, F2, and F1), which affect the flue gas extraction rate whilst maintaining the same intermediate auger speed. Furthermore, the flue gas flow rate (Nm³/h) was calculated via Equation (1):

$$MFR \times \left[\text{Air stoichiometry} \times (\lambda - 0.21) + \frac{(1.85 \times C + 11.09 \times H + 1.24 \times MC + 0.80 \times N + 0.68 \times S)}{100} \right] \quad (1)$$

where *C*, *H*, *N*, *S*, and *MC* refer to the samples' values, and λ corresponds to the ratio of supplied air to the stoichiometry air, with higher values suggesting less efficient combustion.

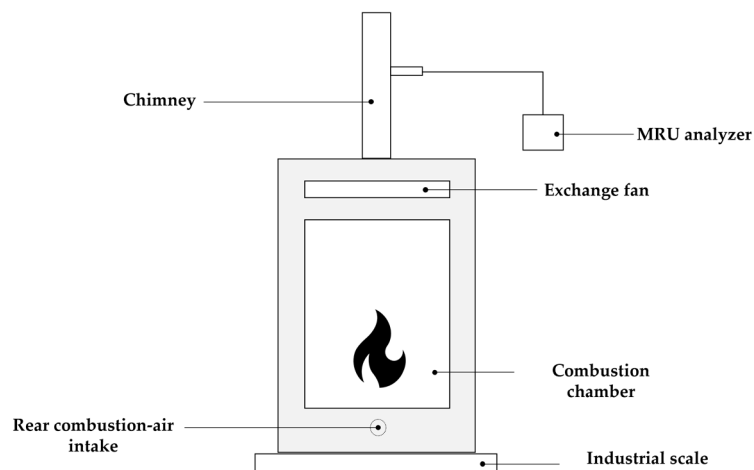


Figure 1. Diagram of the experimental combustion test system.

The amount of combustion air which flows in the combustion chamber is greater in F3 (60% of maximum rpm), intermediate in F2 (53% of maximum rpm), and lower in F1 (47% of maximum rpm). Starting from the NCV and flue gas rates, both the CO and NO_x data were normalized to the fuel's input energy (MJ).

Whilst NO_x mainly depends on two factors, specifically the amount of N in the fuel and the temperature in the combustion chamber that allows for the oxidation of atmospheric nitrogen, CO is a key parameter in the assessment of the combustion efficiency given its correlation with the oxidation of organic carbon in biofuel [32,33]. Therefore, the monitoring of CO and the temperature of flue gasses is crucial in evaluating combustion efficiency.

Preliminary tests were performed to define the optimal timing for proper combustion tests. Specifically, it was found that 45 min allows for stable temperature to be reached inside the combustion chamber, evaluated on the basis of the constancy of the flue gas temperature. Furthermore, it has been observed that the emission trends stabilized about 20 min after switching stove programs.

Each type of pellet was combustion-tested 5 times, following the same procedure throughout each test, specifically, 1 h of pre-heating with F3; 1 h of data acquisition with F3; 30 min of stabilization with F2; 1 h of data acquisition with F2; 30 min of stabilization with F1; and lastly, 1 h of data acquisition with F1.

2.3. Dimensional Image Processing Analysis

The prototypal DIP system (Figure 2) is made up of (i) a 64 Mp camera placed on a tripod at a height of 150 mm, (ii) a flat 250 × 300 mm container for sample placing, (iii) a 250 lm light source positioned at a 45-degree angle to the sample at 300 mm distance from the sample container, (iv) a Python-based image processing script. The distance of the camera from the sample and camera settings (ISO 400, shutter speed 1/10, focus 0.7 mm) were chosen in order to allow only the sample to be included in the picture, which also had to be as sharpest as possible. The angle and distance of the light source were chosen by observing that a 45-degree angle led to more shadows being cast.

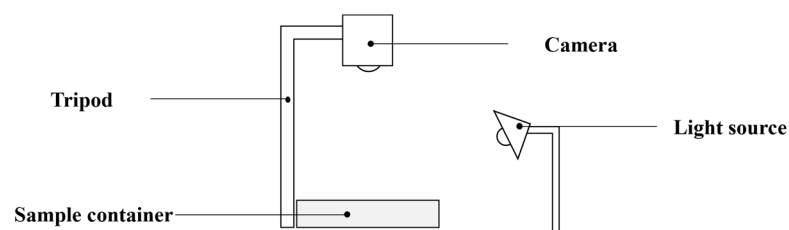


Figure 2. Diagram of the DIP prototypal system.

The DIP analysis requires approximately 2 kg of pellets to be placed in the container, filling the view of the camera completely. Next, the pellets need to be leveled, ensuring that shadows are generated solely by pellet size rather than the samples' bulk height differences.

Subsequent to image acquisition, shadows are highlighted as a result of the application of Otsu's threshold value [34] and binarization of the image. Shadows in contact with the boundaries of the image are excluded given that their exact size cannot be calculated [35]. Data regarding the number and shape of shadows are therefore acquired.

Three pictures were taken for each sub-sample, stirring the pellets in between. Thus, the average data for the Sp2, Mp2, and Lp2 samples were obtained.

2.4. Statistical Analysis

The data obtained from the 5 combustion test replicates conducted with each program were averaged and examined by means of descriptive statistics.

The data collected via DIP analysis were analyzed by means of descriptive statistics, Pearson correlation analysis, and principal component analysis (PCA).

3. Results and Discussions

3.1. Sample Characteristics

The average length and quality parameters of Sp, Mp, and Lp are shown in Table 1.

Table 1. Average data for Sp, Mp, and Lp, where MC corresponds to moisture values; NCV, HCV, and LCV correspond, respectively, to net, higher, and lower calorific values; and Db and L correspond, respectively, to sample durability and average length.

| Sample | MC % w.b. | Ash % d.b. | NCV J/g w.b. | HCV J/g d.b. | LCV J/g d.b. | C % d.b. | H % d.b. | N % d.b. | Cl % d.b. | S % d.b. | Db % | Fines % | L mm |
|--------|--------------|---------------|-----------------|-----------------|-----------------|-------------|-------------|-------------|--------------|-------------|---------|------------|---------|
| Sp | 9.6 | 0.4 | 16,200 | 19,488 | 18,188 | 50.1 | 6.0 | 0.2 | 0.0 | 0.1 | 96.4 | 0.7 | 10.7 |
| Mp | 8.1 | 0.4 | 16,403 | 19,461 | 18,067 | 49.9 | 6.6 | 0.1 | 0.0 | 0.0 | 98.6 | 0.1 | 15.9 |
| Lp | 10.3 | 0.5 | 15,569 | 19,029 | 17,635 | 49.8 | 6.4 | 0.1 | 0.0 | 0.1 | 92.7 | 1.3 | 21.1 |

Distancing the knives from the die successfully led to the production of samples with different length class distributions (Figure 3a). Whilst knife–die distances of 25 mm and 35 mm led to homogeneous samples, increasing the distance to 45 mm led to a more heterogeneous length class distribution. The latter occurrence may be due to the intense vibrations of the pelletizer, which, if the pellets coming out of the die are not durable enough, lead to premature breakage of the pellets.

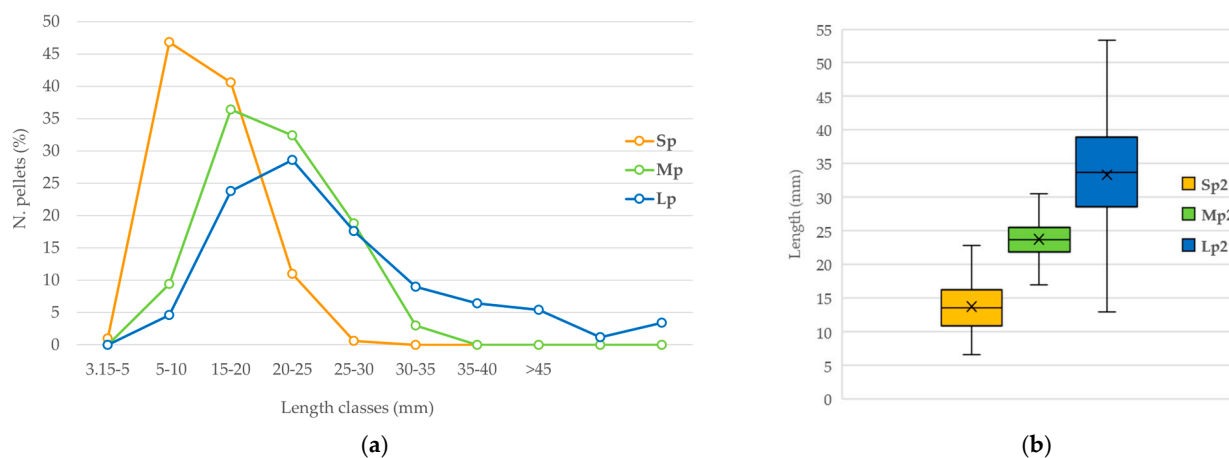


Figure 3. (a) Length class distribution of Sp, Mp, and Lp. (b) Boxplots of Sp2, Mp2, and Lp2.

The sample analyses highlighted some qualitative differences, such as in MC and mechanical durability. While the former may depend on the different degrees of MC

in the pile from which the material was taken for pellet production [11], the latter may depend on both the MC itself and the average length, which, if excessive, makes the pellets fragile [36,37]. Furthermore, lower durability values lead to a higher fine content [12,38]. No differences in chemical composition and energetic content have been observed.

Lastly, boxplots of Sp2, Mp2, and Lp2 are shown in Figure 3b, highlighting the clear difference in lengths between the samples used for the DIP analysis. Specifically, their average lengths were 13.8 mm for Sp2, 23.7 mm for Mp2, and 33.3 for Lp2.

3.2. Combustion Tests' Results

Using the same intermediate auger speed for combustion tests demonstrated the inverse relationship between samples' length and MFR ($R^2 = 0.95$). Specifically, the Sp sample was characterized by an average consumption of 1.71 kg/h, whilst Mp and Lp were characterized, respectively, by average consumptions of 1.59 kg/h and 1.32 kg/h.

Table 2 displays the average data obtained from the five combustion test replicates prior to normalization, whilst average normalized trends in CO (mg/MJ) observed during the F3, F2, and F1 programs are shown in Figure 4.

Table 2. Averaged data from 5 combustion test replicates prior to normalization. Standard deviations are given in brackets.

| Sample | F3 | | F2 | | F1 | | | | | | | |
|--------|----------------|-----------|----------------------|-----------------------|----------------|-----------|----------------------|-----------------------|----------------|-----------|----------------------|-----------------------|
| | Gas °C | λ | CO mg/m ³ | NOx mg/m ³ | Gas °C | λ | CO mg/m ³ | NOx mg/m ³ | Gas °C | λ | CO mg/m ³ | NOx mg/m ³ |
| Sp | 179 (2.3) | 4.4 | 230.5 (73) | 129.1 (13.5) | 173.6 (1.6) | 3.7 | 217 (58.5) | 147.3 (15.4) | 165.1 (1.3) | 3.2 | 209.6 (51.7) | 159.5 (18.9) |
| Mp | 174.9 (2.7) | 4.8 | 225.9 (122.8) | 77.9 (11.1) | 168.9 (2) | 4 | 215.9 (90.9) | 87.8 (12.4) | 161.5 (2.0) | 3.5 | 215.8 (76.9) | 93.8 (13) |
| Lp | 169.8 (3.6) | 5.6 | 354.4 (190.1) | 73.8 (13.1) | 165.5 (2.9) | 4.8 | 336.4 (178) | 81.4 (14.3) | 159.7 (2.3) | 4 | 324.2 (122.2) | 90.9 (14.9) |

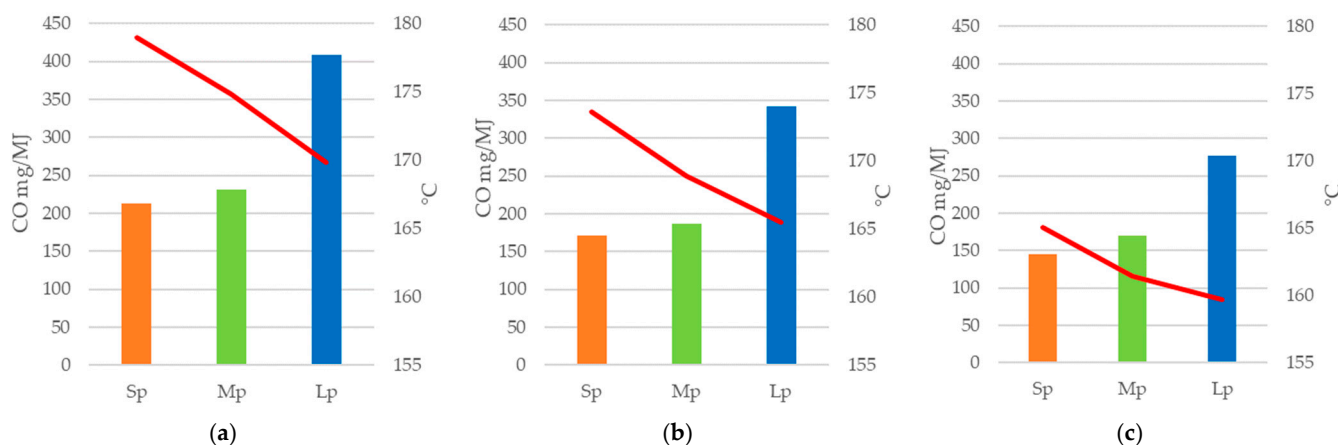


Figure 4. Average normalized CO data (mg/MJ) from 5 combustion tests. Each colored bin represents a different sample, whilst the red line represents the average temperature of flue gases obtained during (a) program F3, (b) program F2, and (c) program F1.

When compared to the other samples, Sp led to lower CO production for each stove program. In fact, the average Sp data between programs highlighted 12% and 94% lower production of CO (mg/MJ) when compared to Mp and Lp, respectively. Furthermore, a better combustion efficiency of Sp was also highlighted by the lower λ values, which indicates less excess air and, thus, more efficient combustion [32]. For example, during program F3, Lp led to 5.6 λ and Mp to 4.8 λ , while Sp led to 4.4 λ . An overall reduction in

CO and λ values was observed by decreasing the combustion-air inlet (switching from F3 to F2 and lastly to F1).

Thus, increasing pellet length affected not only MFR but also combustion efficiency [16]. This might be because less of the surface area of longer pellets is in direct contact with combustion air compared with that in shorter pellets. Additionally, the more uniform spatial arrangement of the shorter pellets in the brazier could have improved the mixing between fuel and combustion air, resulting in more efficient oxidation of CO [17,39,40]. On the contrary, a more heterogeneous spatial arrangement of pellets, which could occur with irregular samples such as Lp (Figure 3a), might have generated voids in the brazier, leading to an excessively rapid flow of combustion air through the fuel bed. This condition leads to shorter residence time of the gaseous combustion products in the high-temperature zone of the flame, negatively affecting the combustion kinetics and carbon oxidation [32]. This could explain the reason why program F1 (Figure 4c) with lower combustion-air flow led to less overall CO emissions.

Flue gas temperatures followed the same trend in all programs. Sp produced higher temperatures when compared to Mp and Lp, given its higher MFR [41]. The highest gas temperatures were obtained during program F3 (Figure 4a), and it may have been due to the shorter residence time of the flue gasses in the system, which allowed for less heat exchange with the system's components and greater heat loss in the chimney. Further studies should investigate thermal trends directly in the combustion chamber.

The average trends in NO_x (mg/MJ) observed during the F3, F2, and F1 programs are shown in Figure 5. Whilst CO emissions are related to the stoichiometry of combustion [32], NO_x emissions strongly depend on the biomasses' N content [42–44] and MFR (i.e., on the N-fuel fed to the combustion process). The Sp sample, being the one with higher MFR and N contents (0.2% d.b.), led to higher NO_x emissions compared to Mp and Lp. Sp's higher NO_x emissions might also depend on the higher temperatures generated during combustion. That is, at temperatures greater than 1300 °C, which could occur in some areas of the flame, thermal NO_x is generated via the oxidation of atmospheric N [32,45,46].

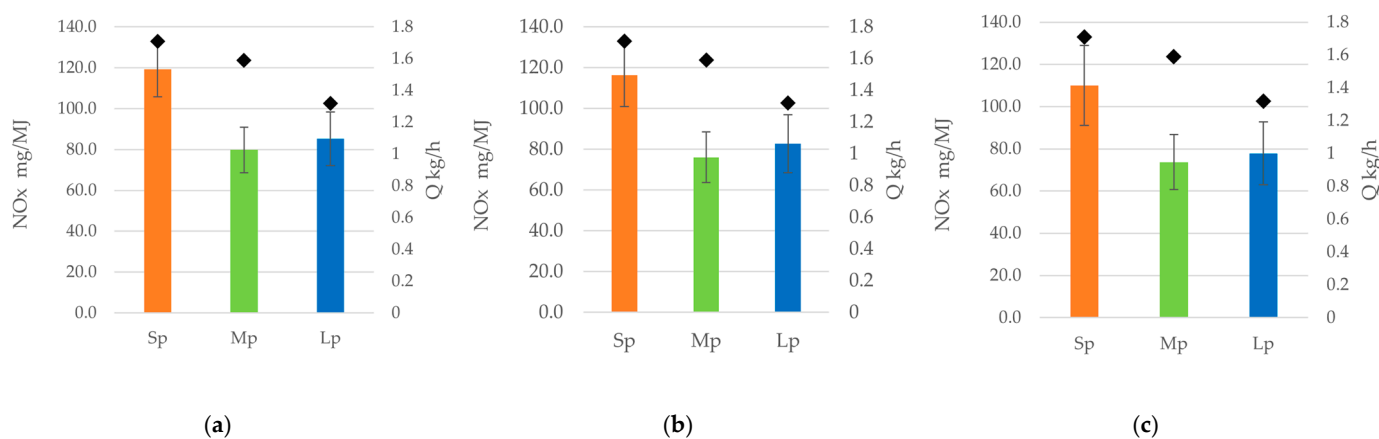


Figure 5. Average normalized NO_x data (mg/MJ) from 5 combustion tests during the (a) F3, (b) F2, and (c) F1 programs. Each colored bin represents a different sample, the bars represent standard deviation, and the black dots represent the MFR of each sample.

The F1 program led to a slight decrease in NO_x emissions, whilst however representing the program with the most variable NO_x emissions (Figure 5c).

3.3. DIP Analysis

An extract of the processed images obtained via the DIP analysis are shown in Figure 6, whilst Table 3 reports the average data and descriptive statistics of the processed images, specifically the number of shadows or objects detected (Obj), the number of pixels contained in the objects (Area), the number of pixels contained in the bounding box tangent to the

outermost pixels of objects (Bbx), the solidity or ratio of pixels in the region to pixels in the convex hull image (Sol), and the eccentricity or elongation of the objects (Ec) [47–49].

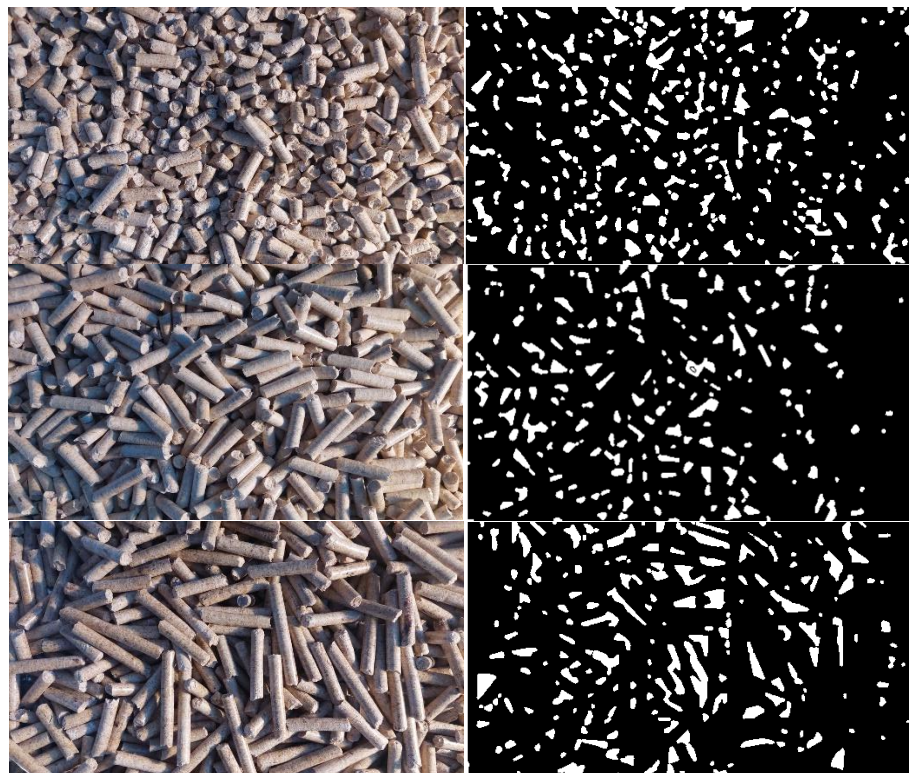


Figure 6. An extract of the images taken via DIP. The shorter pellet, Sp2, produced more but smaller shadows compared to the longer pellet Lp2.

Table 3. Average DIP data indicating the number of shadows or objects detected (Obj), the number of pixels contained in the objects (Area), the number of pixels contained in the bounding box tangent to the outermost pixels of objects (Bbx), the solidity or ratio of pixels in the region to pixels in the convex hull image (Sol), and the eccentricity or elongation of the objects (Ec).

| | Sp2 | | | | | Mp2 | | | | | Lp2 | | | | |
|----------|-----|------|--------|------|------|-----|------|------|------|------|-----|------|--------|------|------|
| | Obj | Area | Bbx | Sol | Ec | Obj | Area | Bbx | Sol | Ec | Obj | Area | Bbx | Sol | Ec |
| N. | 879 | | | | | 669 | | | | | 643 | | | | |
| Mean | | 276 | 632 | 0.87 | 0.80 | | 321 | 702 | 0.89 | 0.83 | | 502 | 1236 | 0.87 | 0.85 |
| St. Dev. | | 305 | 1062 | 0.11 | 0.14 | | 342 | 985 | 0.09 | 0.14 | | 598 | 1892 | 0.11 | 0.14 |
| Min | | 30 | 35 | 0.38 | 0.15 | | 30 | 35 | 0.42 | 0.27 | | 30 | 35 | 0.35 | 0.17 |
| Q1 25% | | 79 | 120 | 0.84 | 0.73 | | 92 | 143 | 0.86 | 0.75 | | 106 | 168 | 0.83 | 0.78 |
| Q2 50% | | 169 | 285 | 0.91 | 0.83 | | 201 | 364 | 0.92 | 0.87 | | 285 | 532 | 0.90 | 0.88 |
| Q3 75% | | 351 | 725 | 0.94 | 0.91 | | 436 | 819 | 0.94 | 0.94 | | 661 | 1458 | 0.94 | 0.95 |
| Max | | 1961 | 11,252 | 1.00 | 0.99 | | 2841 | 8586 | 1.00 | 0.99 | | 4410 | 17,018 | 1.00 | 0.99 |

A negative correlation was observed between the average length of the samples and Obj ($R^2 = -0.91$). In contrast, positive correlations were found between length and Area ($R^2 = 0.94$) and length and Bbx ($R^2 = 0.90$). The strongest correlation was between length and Ec ($R^2 = 0.99$), while the weakest was between length and Sol ($R^2 = -0.22$).

Interquartile ranges (IQR) indicate a less spread-out middle half distribution of Area in Sp2 (IQR = 272), compared to Mp2 (IQR = 344) and Lp2 (IQR = 555). Furthermore, a positive correlation between IQR and average samples' length ($R^2 = 0.92$). Sp2 also led to a smaller range, the difference between the maximum and minimum Area values (range = 1931), compared to Mp2 (range = 2811) and Lp2 (range = 4380).

Figure 7 highlights the distribution of Area data grouped by area class of each sample. Among the classes, the first and smallest appear to be the most distinctive. Specifically, the averaged data of Sp2 led to more than 531 objects falling within the first class (30–230 Area), compared to Mp2 and Lp2 with, respectively, 362 and 284 objects falling within the first class.

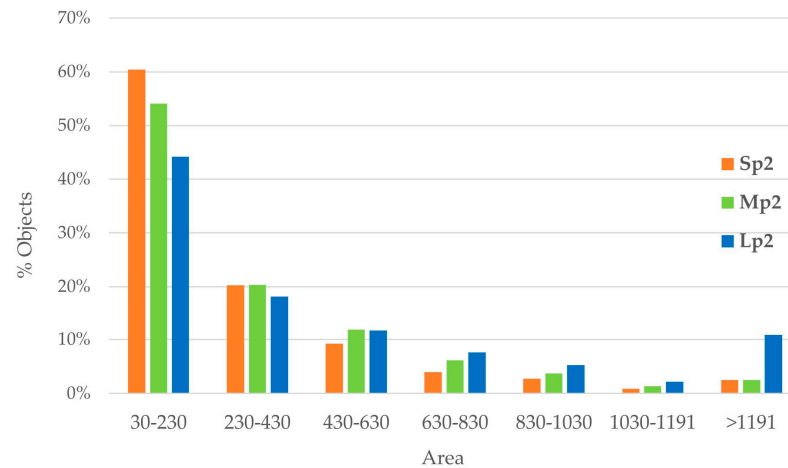


Figure 7. Distribution of objects detected via DIP in terms of Area classes.

PCA's biplot further emphasized the inverse relation between sample length and Obj, as well as the positive relation between length and Ec (Figure 8).

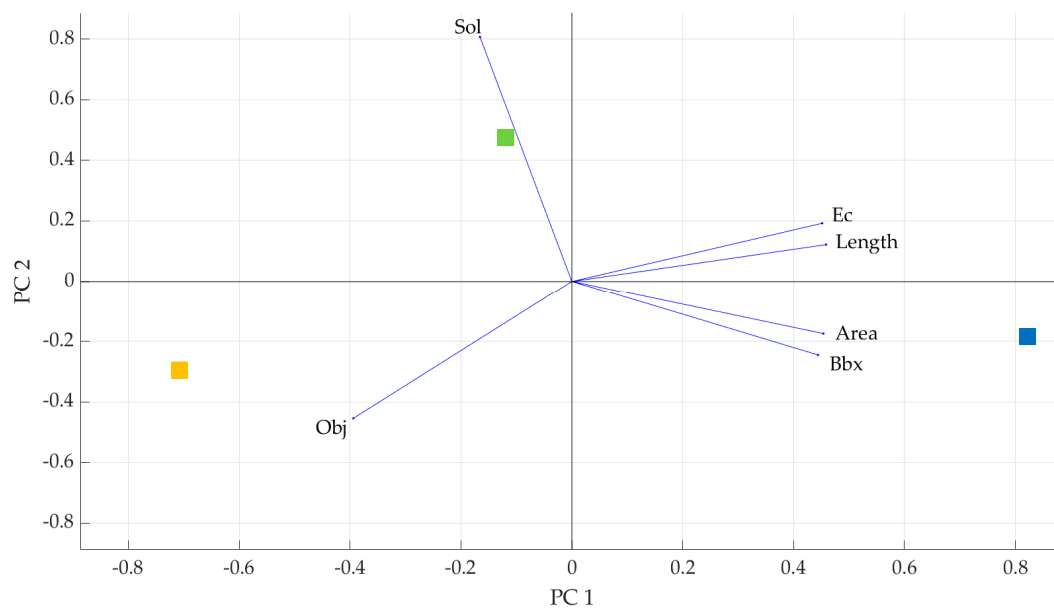


Figure 8. Biplots highlighting a difference between samples and confirming the inverse relationship between sample length and the number of objects detected via DIP analysis. The orange square corresponds to Sp2, the green square corresponds to Mp2, and the blue square corresponds to Lp2.

Lastly, a Pearson analysis (Table 4) indicated Ec as most related output variable to sample length ($r = 1$). However, all other variables appear to be highly correlated with average sample length.

Table 4. Pearson analysis shows a strong correlation between length and Obj, Area, and Ec, with the latter being the most strongly correlated.

| | Length | Obj | Area | Bbx | Ec | Sol |
|--------|--------|-------|-------|-------|-------|-----|
| Length | 1 | | | | | |
| Obj | −0.92 | 1 | | | | |
| Area | 0.94 | −0.73 | 1 | | | |
| Bbox | 0.91 | −0.67 | 1.00 | 1 | | |
| Ec | 1.00 | −0.95 | 0.91 | 0.87 | 1 | |
| Sol | −0.22 | −0.19 | −0.54 | −0.61 | −0.14 | 1 |

4. Conclusions

By producing pellet samples from the same raw material taken from the same pile, whilst varying the distance of the knife from the die during production, it was possible to obtain samples that were qualitatively similar but with different dimensional parameters. Thus, three pellet samples with different average lengths (short—Sp, medium—Mp, and long—Lp) were produced and tested in a domestic pellet stove in order to confirm the effect of pellet length on combustion efficiency [16,17].

Under equal stove conditions (auger feeding rate and flue gas extractor rate), Lp emitted up to 83% more CO mg/MJ than Mp and 99% more CO mg/MJ compared to Sp. On the contrary, pellet length appeared to be negatively correlated with NOx emissions (Sp produced up to 29% more NOx when compared to Lp). Specifically, different pellet lengths are associated with different mass flow rates with the same auger feed rate, leading to a variation in lambda values (less efficiency and higher CO emissions) and amount of N-fuel supplied to the combustion process (NOx emissions) [32].

Furthermore, sample length and MFR also affected the temperatures of flue gasses, being higher in Sp compared to Mp and Lp, regardless of the combustion-air inlet.

Given the high importance of pellet length in combustion quality and the impracticability of ISO 17829 outside laboratory measurements, an innovative prototype based on image processing (DIP) to assess samples' average length has been developed. The DIP method assumes that larger pellets, when subjected to transversal illumination, generate geometrically and quantitatively different shadows from shorter pellets. By analyzing shadows rather than applying segmentations directly on pellets, DIP provides a solution to measurement errors caused by the inability of image processing techniques to easily detect objects that are not perpendicular to the camera. Furthermore, image processing methods generally require a metric reference with which to make a comparison between the photographed object and the reference with known dimensions.

An inverse relation between sample length and the number of detected shadows has been found. Specifically, Sp2 led to the formation of 24% more shadows compared to Mp2 and 26% more than Lp2. In contrast, the average size of the shadows appeared to be inversely correlated with sample length. Lastly, a Pearson analysis highlighted eccentricity, which is the ratio of the distance between furthest pixels that make up objects, as the variable most correlated with sample length.

Currently, domestic stoves do not have an automatic system to control combustion due to the high cost of components (e.g., lambda sensors), which would make the system non-competitive on the market. The proposed approach could potentially translate into the implementation of a simple and low-cost camera that communicates with the programmable control unit (already installed in commercialized stoves) and automatically sets the auger speed or flue gas extractor to reduce emissions and increase thermal efficiency. Furthermore, a camera installed on the stove could also have other valuable applications for processing pellets, such as detecting hazardous objects on the auger or monitoring the number of pellets left in the hopper.

This paper lays the groundwork for future research, which should test DIP on a larger number of samples and model the relationship between the shadows and sample length class distributions. Furthermore, it may be necessary to test the effect of different

light angles on the formation of shadows. Lastly, by extensively assessing DIP performance, it could also be used as a viable alternative to the traditional system for the online measurement of bulk density in pellet production plants.

5. Patents

The method for analyzing the dimensional class of objects by examining the shadows cast by objects arranged in groups or in bulk (referred to in this document as DIP) is the subject of a pending patent. The pending patent No. 102024000017878 dated 31/07/2024 has been submitted to the Italian Patent and Trademark Office—UIBM and is titled “Computer-implemented method for the analysis of the dimensional class of objects”.

Author Contributions: Conceptualization, G.T. and D.D.; methodology, T.G.; software, A.P.; validation, D.D., T.G. and A.P.; formal analysis, T.G.; investigation, G.T. and A.I.; resources, G.T. and D.D.; data curation, D.D., T.G. and A.P.; writing—original draft preparation, T.G. and L.O.; writing—review and editing, A.I., D.D., T.G. and A.P.; visualization, T.G., A.I. and L.O.; supervision, G.T.; project administration, D.D. and G.T.; funding acquisition, G.T. All authors have read and agreed to the published version of the manuscript.

Funding: This research received no external funding.

Data Availability Statement: The data presented in this study are available from the corresponding authors on request. The data are not publicly available due to being part of a pending patent.

Acknowledgments: A special thanks to Enerlegno for their support in the production of the pellet samples.

Conflicts of Interest: The authors declare no conflicts of interest.

References

1. European Commission. A Green Deal Industrial Plan for the Net-Zero Age. COM (2023) 62, ch II. Available online: <https://eur-lex.europa.eu/legal-content/EN/TXT/?uri=CELEX:52023DC0062> (accessed on 1 November 2024).
2. Thomson, H.; Liddell, C. The Suitability of Wood Pellet Heating for Domestic Households: A Review of Literature. *Renew. Sustain. Energy Rev.* **2015**, *42*, 1362–1369. [[CrossRef](#)]
3. Sikkema, R.; Steiner, M.; Junginger, M.; Hiegl, W.; Hansen, M.T.; Faaij, A. The European Wood Pellet Markets: Current Status and Prospects for 2020. *Biofuels Bioprod. Biorefining* **2011**, *5*, 250–278. [[CrossRef](#)]
4. Mola-Yudego, B.; Selkimäki, M.; González-Olabarria, J.R. Spatial Analysis of the Wood Pellet Production for Energy in Europe. *Renew. Energy* **2014**, *63*, 76–83. [[CrossRef](#)]
5. Eurostat Data Browser. Roundwood, Fuelwood and Other Basic Products. Available online: <https://ec.europa.eu/eurostat/databrowser> (accessed on 29 November 2024).
6. Piazzalunga, A.; Anzano, M.; Collina, E.; Lasagni, M.; Lollobrigida, F.; Pannocchia, A.; Fermo, P.; Pitea, D. Contribution of Wood Combustion to PAH and PCDD/F Concentrations in Two Urban Sites in Northern Italy. *J. Aerosol Sci.* **2013**, *56*, 30–40. [[CrossRef](#)]
7. Gualtieri, G.; Crisci, A.; Tartaglia, M.; Toscano, P.; Vagnoli, C.; Andreini, B.P.; Gioli, B. Analysis of 20-Year Air Quality Trends and Relationship with Emission Data: The Case of Florence (Italy). *Urban. Clim.* **2014**, *10*, 530–549. [[CrossRef](#)]
8. ISO 17225-2:2021; Solid Biofuels—Fuel Specifications and Classes—Part 2: Graded Wood Pellets. ISO: Geneva, Switzerland, 2021.
9. ISO 17829:2015; Solid Biofuels—Determination of Length and Diameter of Pellets. ISO: Geneva, Switzerland, 2015.
10. Jägers, J.; Wirtz, S.; Scherer, V. An Automated and Continuous Method for the Optical Measurement of Wood Pellet Size Distribution and the Gravimetric Determination of Fines. *Powder Technol.* **2020**, *367*, 681–688. [[CrossRef](#)]
11. Toscano, G.; Leoni, E.; Feliciangeli, G.; Duca, D.; Mancini, M. Application of ISO Standards on Sampling and Effects on the Quality Assessment of Solid Biofuel Employed in a Real Power Plant. *Fuel* **2020**, *278*, 118142. [[CrossRef](#)]
12. Gilvari, H.; de Jong, W.; Schott, D.L. The Effect of Biomass Pellet Length, Test Conditions and Torrefaction on Mechanical Durability Characteristics According to ISO Standard 17831-1. *Energy* **2020**, *13*, 3000. [[CrossRef](#)]
13. Lisowski, A.; Matkowski, P.; Dąbrowska, M.; Piątek, M.; Świętochowski, A.; Klonowski, J.; Mieszkalski, L.; Reshetiuk, V. Particle Size Distribution and Physicochemical Properties of Pellets Made of Straw, Hay, and Their Blends. *Waste Biomass Valorization* **2020**, *11*, 63–75. [[CrossRef](#)]
14. Pradhan, P.; Arora, A.; Mahajani, S.M. Factors Affecting the Quality of Fuel Pellets Produced from Waste Biomass. *IOP Conf. Ser. Earth Environ. Sci.* **2020**, *463*, 012013. [[CrossRef](#)]
15. Obaidullah, M.; Bram, S.; Verma, V.K.; De Ruyck, J. A Review on Particle Emissions from Small Scale Biomass Combustion. *Int. J. Renew. Energy Res.* **2012**, *2*, 147–159.
16. Wöhler, M.; Jaeger, D.; Reichert, G.; Schmidl, C.; Pelz, S.K. Influence of Pellet Length on Performance of Pellet Room Heaters Under Real Life Operation Conditions. *Renew. Energy* **2017**, *105*, 66–75. [[CrossRef](#)]

17. Mack, R.; Schön, C.; Kuptz, D.; Hartmann, H.; Brunner, T.; Obernberger, I.; Behr, H.M. Influence of Pellet Length, Content of Fines, and Moisture Content on Emission Behavior of Wood Pellets in a Residential Pellet Stove and Pellet Boiler. *Biomass Convers. Biorefin.* **2022**, *14*, 26827–26844. [CrossRef]
18. Dahal, K.; Tissari, J.; Hartmann, H.; Schön, C.; Fraboulet, I.; Cea, B.; Kubesa, P.; Horak, J. Technical Report on Review of Particulate Emissions Produced from the Small-Scale Solid Fuel Combustion. 2022. Available online: https://www.researchgate.net/profile/Karna-Dahal/publication/374472110_Technical_report_on_review_of_particulate_emissions_produced_from_the_small-scale_solid_fuel_combustion/links/651f0b813ab6cb4ec6bdf517/Technical-report-on-review-of-particulate-emissions-produced-from-the-small-scale-solid-fuel-combustion.pdf?_tp=eyJjb250ZXh0Ijp7ImZpcnN0UGFnZSI6InB1YmxyY2F0aW9uIiwicGFnZSI6InB1YmxyY2F0aW9uIn19 (accessed on 2 November 2024).
19. Igathinathane, C.; Melin, S.; Sokhansanj, S.; Bi, X.; Lim, C.J.; Pordesimo, L.O.; Columbus, E.P. Machine Vision Based Particle Size and Size Distribution Determination of Airborne Dust Particles of Wood and Bark Pellets. *Powder Technol.* **2009**, *196*, 202–212. [CrossRef]
20. Chaloupková, V.; Ivanova, T.; Ekrt, O.; Kabutey, A.; Herák, D. Determination of Particle Size and Distribution Through Image-Based Macroscopic Analysis of the Structure of Biomass Briquettes. *Energy* **2018**, *11*, 331. [CrossRef]
21. Pierdicca, R.; Balestra, M.; Micheletti, G.; Felicetti, A.; Toscano, G. Semi-Automatic Detection and Segmentation of Wooden Pellet Size Exploiting a Deep Learning Approach. *Renew. Energy* **2022**, *197*, 406–416. [CrossRef]
22. Toscano, G.; Leoni, E.; De Francesco, C.; Ciccone, G.; Gasperini, T. The Application of Image Acquisition and Processing Techniques for the Determination of Wooden Pellet Length as an Alternative to ISO 17829. *Resources* **2023**, *12*, 125. [CrossRef]
23. Ozgen, S.; Caserini, S.; Galante, S.; Giugliano, M.; Angelino, E.; Marongiu, A.; Hugony, F.; Migliavacca, G.; Morreale, C. Emission Factors from Small Scale Appliances Burning Wood and Pellets. *Atmos. Environ.* **2014**, *94*, 144–153. [CrossRef]
24. ISO 21945:2020; Solid Biofuels—Simplified Sampling Method for Small Scale Applications. ISO: Geneva, Switzerland, 2020.
25. ISO 18134-2:2024; Solid Biofuels—Determination of Moisture Content. Part 2: Simplified Method. ISO: Geneva, Switzerland, 2024.
26. ISO 18122:2022; Solid Biofuels—Determination of Ash Content. ISO: Geneva, Switzerland, 2022.
27. ISO 18125:2017; Solid Biofuels—Determination of Calorific Value. ISO: Geneva, Switzerland, 2017.
28. ISO 16948:2015; Solid Biofuels—Determination of Total Content of Carbon, Hydrogen and Nitrogen. ISO: Geneva, Switzerland, 2015.
29. ISO 16994:2016; Solid Biofuels—Determination of Total Content of Sulfur and Chlorine. ISO: Geneva, Switzerland, 2016.
30. ISO 17831-1:2015; Solid Biofuels—Determination of Mechanical Durability of Pellets and Briquettes. Part 1: Pellets. ISO: Geneva, Switzerland, 2015.
31. ISO 18846:2016; Solid Biofuels—Determination of Fines Content in Quantities of Pellets. ISO: Geneva, Switzerland, 2016.
32. van Loo, S.; Koppejan, J. *The Handbook of Biomass Combustion and Co-Firing*; Earthscan: Oxford, UK, 2012; pp. 1–442. [CrossRef]
33. Arranz, J.I.; Miranda, M.T.; Montero, I.; Sepúlveda, F.J.; Rojas, C.V. Characterization and Combustion Behaviour of Commercial and Experimental Wood Pellets in South West Europe. *Fuel* **2015**, *142*, 199–207. [CrossRef]
34. Otsu, N. Threshold Selection Method from Gray-Level Histograms. *IEEE Trans. Syst. Man. Cybern.* **1979**, *SMC-9*, 62–66. [CrossRef]
35. Oh, S.M.; Park, J.; Yang, J.; Oh, Y.G.; Yi, K.W. Image Processing for Analysis of Carbon Black Pellet Size Distribution During Pelletizing: Carbon Black PSD (PSD: Pellet Size Distribution) by Image Processing. *Measurement* **2021**, *174*, 108963. [CrossRef]
36. Nimitpaitoon, T.; Sajjakulnukit, B. Study on the Effects of Storage Conditions on Pretreated and Raw Biomass. *Int. J. Adv. Appl. Sci.* **2022**, *9*, 136–144. [CrossRef]
37. Whittaker, C.; Shield, I. Factors Affecting Wood, Energy Grass and Straw Pellet Durability—A Review. *Renew. Sustain. Energy Rev.* **2017**, *71*, 1–11. [CrossRef]
38. García-Maraver, A.; Popov, V.; Zamorano, M. A Review of European Standards for Pellet Quality. *Renew. Energy* **2011**, *36*, 3537–3540. [CrossRef]
39. Yazdanpanah, F.; Sokhansanj, S.; Lau, A.K.; Lim, C.J.; Bi, X.; Melin, S. Airflow Versus Pressure Drop for Bulk Wood Pellets. *Biomass Bioenergy* **2011**, *35*, 1960–1966. [CrossRef]
40. Thunman, H.; Leckner, B. Influence of Size and Density of Fuel on Combustion in a Packed Bed. *Proc. Combust. Inst.* **2005**, *30*, 2939–2946. [CrossRef]
41. Cahyo, N.; Alif, H.H.; Aditya, I.A.; Saksono, H.D. Co-Firing Characteristics of Wood Pellets on Pulverized Coal Power Plant. *IOP Conf. Ser. Mater. Sci. Eng.* **2021**, *1098*, 062088. [CrossRef]
42. Stubenberger, G.; Scharler, R.; Zahirović, S.; Obernberger, I. Experimental Investigation of Nitrogen Species Release from Different Solid Biomass Fuels as a Basis for Release Models. *Fuel* **2008**, *87*, 793–806. [CrossRef]
43. Johansson, L.S.; Leckner, B.; Gustavsson, L.; Cooper, D.; Tullin, C.; Potter, A. Emission Characteristics of Modern and Old-Type Residential Boilers Fired with Wood Logs and Wood Pellets. *Atmos. Environ.* **2004**, *38*, 4183–4195. [CrossRef]
44. Obernberger, I. Decentralized Biomass Combustion: State of the Art and Future Development. *Biomass Bioenergy* **1998**, *14*, 33–56. [CrossRef]
45. Zheng, S.; Yang, Y.; Li, X.; Liu, H.; Yan, W.; Sui, R.; Lu, Q. Temperature and Emissivity Measurements from Combustion of Pine Wood, Rice Husk and Fir Wood Using Flame Emission Spectrum. *Fuel Process. Technol.* **2020**, *204*, 106423. [CrossRef]
46. Li, J.; Biagini, E.; Yang, W.; Tognotti, L.; Blasiak, W. Flame Characteristics of Pulverized Torrefied-Biomass Combusted with High-Temperature Air. *Combust. Flame* **2013**, *160*, 2585–2594. [CrossRef]
47. Matsuoka, R.; Maruyama, S. Eccentricity on an Image Caused by Projection of a Circle and a Sphere. *ISPRS Ann. Photogramm. Remote Sens. Spat. Inf. Sci.* **2016**, *3*, 19–26. [CrossRef]

48. Kumar, P.; Belchamber, E.R.; Miklavcic, S.J. Pre-Processing by Data Augmentation for Improved Ellipse Fitting. *PLoS ONE* **2018**, *13*, e0196902. [[CrossRef](#)]
49. Di, Y.; Li, M.Y.; Qiao, T.; Lu, N. Edge Detection and Mathematic Fitting for Corneal Surface with Matlab Software. *Int. J. Ophthalmol.* **2017**, *10*, 336–342. [[CrossRef](#)]

Disclaimer/Publisher’s Note: The statements, opinions and data contained in all publications are solely those of the individual author(s) and contributor(s) and not of MDPI and/or the editor(s). MDPI and/or the editor(s) disclaim responsibility for any injury to people or property resulting from any ideas, methods, instructions or products referred to in the content.